Thermal Decomposition of Gaseous Ammonium Nitrate at Low Pressure: Kinetic Modeling of Product Formation and Heterogeneous Decomposition of Nitric Acid

J. Park* and M. C. Lin*

Department of Chemistry, Emory University, Atlanta, Georgia 30322

Received: June 19, 2009; Revised Manuscript Received: September 29, 2009

The thermal decomposition of ammonium nitrate, NH_4NO_3 (AN), in the gas phase has been studied at 423−56 K by pyrolysis/mass spectrometry under low-pressure conditions using a Saalfeld reactor coated with boric acid. The sublimation of NH_4NO_3 at 423 K was proposed to produce equal amounts of NH_3 and HNO_3, followed by the decomposition reaction of HNO_3, $HNO_3 + M \rightarrow OH + NO_2 + M$ (where M = third-body and reactor surface). The absolute yields of N_2, N_2O, H_2O, and NH_3, which can be unambiguously measured and quantitatively calibrated under a constant pressure at 5−6.2 torr He are kinetically modeled using the detailed [H,N,O]-mechanism established earlier for the simulation of NH_3-NO_2 (Park, J.; Lin, M. C. Technologies and Combustion for a Clean Environment. *Proc. 4th Int. Conf.* **1997**, *34-1*, 1−5) and ADN decomposition reactions (Park, J.; Chakraborty, D.; Lin, M. C. *Proc. Combust. Inst*. **1998**, *27*, 2351−2357). Since the homogeneous decomposition reaction of HNO_3 itself was found to be too slow to account for the consumption of reactants and the formation of products, we also introduced the heterogeneous decomposition of HNO_3 in our kinetic modeling. The heterogeneous decomposition rate of HNO_3, $HNO_3 + (B_2O_3/SiO_2) \rightarrow OH + NO_2 + (B_2O_3/SiO_2)$, was determined by varying its rate to match the modeled result to the measured concentrations of NH_3 and H_2O; the rate could be represented by $k_{2b} = 7.91 \times 10^7 \exp(-12\,600/T)$ s^{-1}, which appears to be consistent with those reported by Johnston and co-workers (Johnston, H. S.; Foering, L.; Tao, Y.-S.; Messerly, G. H. *J. Am. Chem. Soc.* **1951**, *73*, 2319-2321) for HNO_3 decomposition on glass reactors at higher temperatures. Notably, the concentration profiles of all species measured could be satisfactorily predicted by the existing [H,N,O]-mechanism with the heterogeneous initiation process.

Introduction

Ammonium nitrate (AN, NH_4NO_3) is a convenient source of N_2O for laboratory experiments. The mechanism for N_2O formation in the melt of AN is believed to involve primarily the reaction of ammonium with nitrate ions.[1]

$$NH_4NO_3(l) \rightarrow NH_4^+ + NO_3^-$$

$$NH_4^+ + NO_3^- \rightarrow NH_3OH^+ + NO_2^-$$

$$NH_3OH^+ + NO_2^- \rightarrow 2HNO + H_2O \rightarrow \mathbf{N_2O} + 2H_2O$$

$$\rightarrow H_2N_2O_2 + H_2O \rightarrow \mathbf{N_2O} + 2H_2O$$

Under higher temperature and particularly low-pressure conditions, contributions from gas-phase reactions become significant.[2] In the gas phase the decomposition of NH_4NO_3 is clearly dominated by the simple dissociation into the acid and base components, most likely similar to the decomposition of the ADN (ammonium dinitramide) system at low pressure:[3]

$$NH_4NO_3(s) \rightarrow NH_3(g) + HNO_3(g)$$

$$HNO_3 \rightarrow OH + NO_2$$

$$OH + NH_3 \rightarrow NH_2 + H_2O$$

$$NH_2 + NO_2 \rightarrow H_2NO + NO$$

$$\rightarrow N_2O + H_2O$$

$$NH_2 + NO \rightarrow N_2H + OH$$

$$\rightarrow N_2 + H_2O$$

The mechanism for gas-phase chain reactions is more complex, involving H and OH as key chain carriers with NH_x and NO_x ($x = 1-3$) as major participants in the redox process. Although kinetic studies of AN have been performed by several authors,[1,2,4,5] important mechanistic questions remain unanswered. In an effort to establish and validate a detailed mechanism for reactions of [H,N,O]-containing systems at high temperatures in conjunction with the NH_3-deNOx process[6] as well as the combustion of AN and ADN, we have recently carried out a low-pressure study on the thermal decomposition of AN in a manner similar to that employed in our ADN decomposition study[3] using a quartz flow reactor employed with a molecular beam sampling/mass spectrometer based on the approach of Saalfeld and co-workers.[7] The rates of formation of the products, which can be unambiguously measured and quantitatively calibrated (for example, N_2, N_2O, H_2O, and NH_3) covering 450−956 K under a constant pressure at 5−6.2 torr, He are kinetically modeled using the detailed mechanism established earlier for the simulation of NH_3-NO_2[8] and ADN decomposition reactions.[3] Both experimental and kinetically modeled results are reported herein.

* To whom correspondence should be addressed. Phone: (404) 727-6841. Fax: (404) 727-6586. E-mail: jpark05@emory.edu (J.P.); chemmcl@emory.edu (M.C.L.).

10.1021/jp9058005 CCC: $40.75
Published on Web 10/21/2009

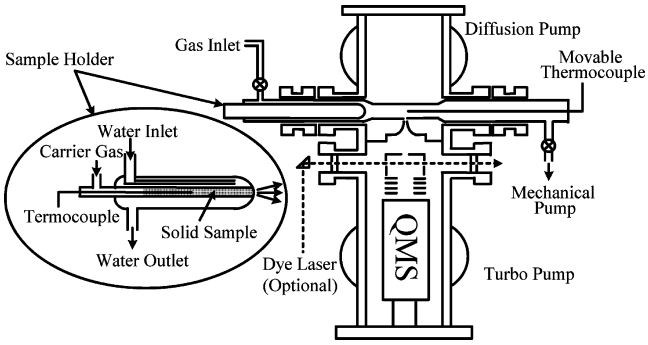

Figure 1. Schematic diagram of the experimental apparatus.

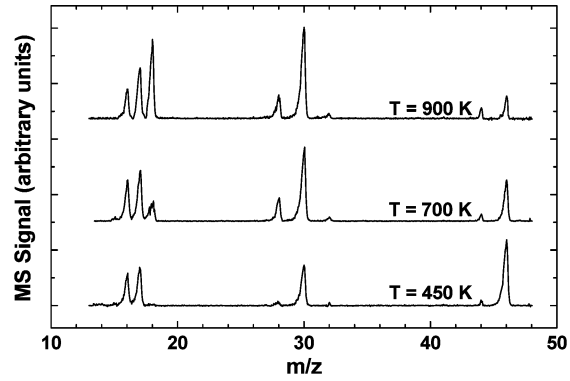

Figure 2. Mass spectra of the AN decomposition products at different reaction temperatures as indicated.

Experimental Procedure

The study of the thermal decomposition reaction of sublimed AN was carried out by using a pyrolysis/mass spectrometric technique in the temperature range 450−956 K. The schematic diagram of the apparatus for the sublimation process and the supersonic mass spectrometric sampling technique is shown in Figure 1.

The sublimation of AN took place in a thermostatted sample holder. In order to achieve homogeneous heating of the sample, we employed continuously circulated hot ethylene glycol−water solution using a NESLAB RTC-110 temperature controller which has an accuracy and reproducibility of 0.3 K. The pyrolysis of the sublimed AN sample entrained with 5−6.2 torr He carrier gas was performed under slow-flow conditions in a Saalfeld-type quartz tubular reactor tube,[7] which has an inner diameter of 10 mm and a length of 140 mm with a conical sampling hole at the center. The reactor was mounted perpendicularly to the detection axis of a quadrupole mass spectrometer (QMS, Extrel model C50), and the reaction tube was wrapped with a 15 mm thick, 15 mm wide Nichrome ribbon and insulated with ceramic wool. The reactor temperature could be varied from 300 to 1000 K by adjusting the current through the heater. In order to minimize heterogeneous surface effects, the inner wall of the reactor was pretreated with boric acid, followed by an extensive bake-out at 1000 K under high vacuum.

The detection chamber housing the mass spectrometer was separated from the supersonic expansion chamber by a metal plate with a 1.0 mm orifice skimmer (Beam Dynamics model 1) mounted at the center of the plate. The supersonically expanded molecular beam was introduced through the skimmer into the ionization region of the spectrometer. The products from the pyrolyzed reaction were supersonically sampled and ionized by electron-impact ionization at 30 eV followed by QMS mass selection. During the experiment, the pressures in the reaction and detection chambers were maintained at $(5-10) \times 10^{-5}$ and $(5-10) \times 10^{-6}$ torr, respectively.

The absolute concentrations of NH_3, N_2, N_2O, and H_2O were calibrated with carefully prepared standard mixtures. The concentration of each individual molecule was obtained by the following formula: $[R] = 9.66 \times 10^{16}$ (%) PF_R/TF_T molecules/cm^3, where % is the percentage of each molecule in its gas mixture, P is the total reaction pressure in torr, T is the reaction temperature, F_R is the flow rate of each gas mixture, and F_T is the total flow rate of all gases. The initial concentration of HNO_3, generated by the sublimation of AN at 423 K, was assumed to be the same as that of NH_3 measured with the reactor temperature set at 450 K, at which no reaction was found to occur.

AN (ammonium nitrate ≥99%, Aldrich), NH_3, H_2O (deionized water), and N_2O were purified by standard trap-to-trap distillation. He and N_2 (99.9995%, UHP, Specialty Gases) were used without further purification. After an AN sample was introduced into the reaction system, it was typically evacuated under high vacuum at room temperature for several days to minimize water contamination.

Results and Discussion

Kinetic Modeling of the AN Decomposition Reaction. Thermal decomposition of AN was studied in the temperature range 450−956 K at total flow rate (F in units of standard cubic centimeter per minute, sccm) of 23 sccm with total pressure of 5 torr or total flow rate of 45 sccm with total pressure of 6.2 torr using He as a carrier gas. The initial reactants were obtained from the sublimation of AN at the constant temperature of 423 K and carried into the preheated Saalfeld reactor at 450 K. The typical mass spectra covering $m/z = 10-50$ obtained at different reactor temperatures are presented in Figure 2. No noticeable peaks beyond $m/z = 50$ were observed within our detectivity. As the reaction does not take place below 450 K in our time scale ($t \leq 40$ ms), the concentration of NH_3 (assumed to be equal to that of HNO_3) and the small traceable amounts of N_2O and N_2 (Figure 2, vide infra) were employed as the initial concentrations of the reactants present for the kinetic modeling of higher temperature results.

The residence (or reaction) time was calculated with the measured flow rate (F in sccm) based on the ideal gas law, t(s) $= (273 \times 60/760)$ (PV/FT), where V is the volume of the reactor in cm^3, P is the total reaction pressure in torr, and T is the reactor temperature in K.

As indicated above, our kinetic modeling was performed with the assumption that $[NH_3]_0 = [HNO_3]_0$, and the reaction was initiated by the decomposition of HNO_3 followed by the chain reactions involving H and OH with NH_x and NO_x ($x = 1-3$):

$$NH_4NO_3(s) \rightarrow NH_3(g) + HNO_3(g) \quad (1)$$

$$HNO_3 + M \rightarrow OH + NO_2 + M \quad (2a)$$

$$HNO_3 + (B_2O_3/SiO_2) \rightarrow OH + NO_2 + (B_2O_3/SiO_2) \quad (2b)$$

$$OH + NH_3 \rightarrow NH_2 + H_2O \quad (3)$$

$$NH_2 + NO_2 \rightarrow H_2NO + NO \quad (4a)$$

$$\rightarrow N_2O + H_2O \quad (4b)$$

$$NH_2 + NO \rightarrow N_2H + OH \quad (5a)$$

$$\rightarrow N_2 + H_2O \quad (5b)$$

For kinetic modeling, we employed 115 reactions which have been utilized in our previous studies of the $NH_x + NO_y$ ($x = 2, 3$; $y = 1, 2$) reactions[8−11] and ADN decomposition reactions.[3] The detailed reaction mechanism is provided in the Supporting Information, and only key reactions employed in the modeling are presented in Table 1. Because the homogeneous initiation reactions, including $HNO_3 + M \rightarrow OH + NO_2 + M$ (2a), $HNO_3 + NH_3 \rightarrow H_2NNO_2 + H_2O$,[12] and other potential processes, were insufficient to account for the consumption of NH_3 and the formation of H_2O, we have to take into consideration the heterogeneous decomposition of HNO_3 (2b) in our kinetic modeling. The initial heterogeneous decomposition of HNO_3 was guided by the decomposition rate of HNO_3 on glass reactors by Johnston and co-workers.[13] Further discussion on the heterogeneous decomposition kinetics and its rate determination will be given in greater detail later with a literature review.

Figure 3 shows our two sets of experimental data with kinetic modeling results. The results of the modeling based on the homogeneous initiation reaction 2a and the heterogeneous initiation reaction 2b are presented by the dashed and solid curves, respectively. The modeled concentrations with the heterogeneous initiation reaction 2b agree reasonably well for the conversion of NH_3 and the growth of H_2O. The other major products were NO and NO_2, but we were not able to differentiate

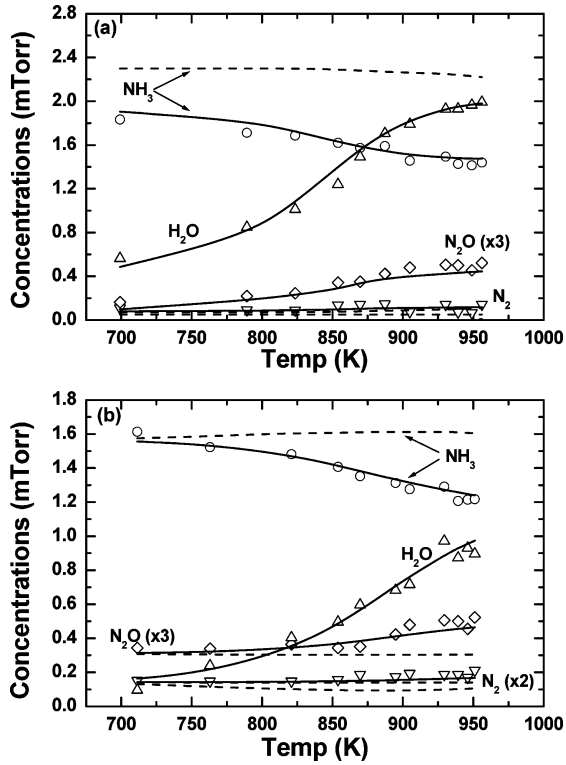

Figure 3. Comparison of experimental data and kinetic modeling results for the sublimed AN decomposition process. Symbols represent experimental data obtained from two different batches of AN samples. Curves are kinetic modeling results with (solid curves) or without (dashed curves) the heterogeneous decomposition of HNO_3. Initial concentrations are (a) $NH_3 = HNO_3 = 2.30$ mtorr, $N_2 = 0.05$ mtorr, residence (reaction) time $= 25.75/T$ s (T in kelvin) and $P = 5.0$ torr with He as carrier gas, (b) $NH_3 = HNO_3 = 1.70$ mtorr, $N_2 = 0.07$ mtorr, $N_2O = 0.10$ mtorr, residence (reaction) time $= 15.16/T$ s (T in kelvin) and $P = 6.2$ torr with He as carrier gas.

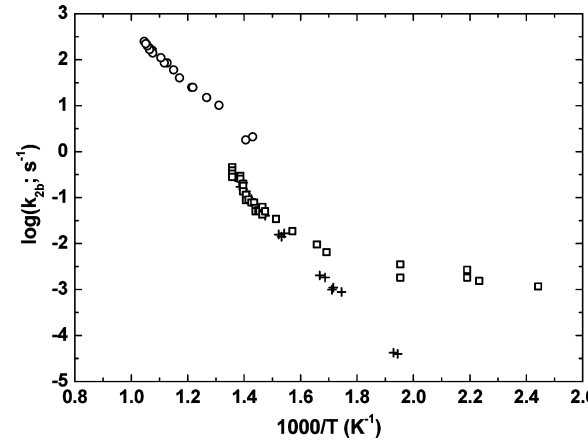

Figure 4. Heterogeneous decomposition reaction rate of nitric acid on the following: ○, 10 mm id and 70 mm length (this work, boric acid coated quartz reactor); □, 6 mm id and 140 mm length (ref 13, glass reactor); +, 25 mm id and 140 mm length (ref 13, glass reactor).

NO and NO_2 peaks at $m/z = 30$ and 46, respectively, from the fragmentation peaks of HNO_3 at $m/z = 30$, 46. Since no noticeable peaks beyond $m/z = 50$ were observed within our detectivity under the experimental conditions, the parent peak of HNO_3 at $m/z = 63$ could not be utilized for kinetic measurements.

Key Elementary Reactions. The gas-phase dissociation reaction of HNO_3 into the NO_2 and OH radicals (2a) and its reverse reaction have been extensively investigated both experimentally[14,15] and theoretically.[16−19] In kinetic modeling we employed our previous work on the HNO_3 decomposition rate which was done by high-level ab initio molecular orbital and statistical theory calculations.[16] The potential energy surfaces have been computed with a modified Gaussian 2 (G2M) method.[20] The rate constant had been calculated by means of the canonical variational RRKM approach. This theoretically predicted rate constant showed reasonably good agreement with the available experimental results, and its rate is represented by $k_{2a} = 4.30 \times 10^3\ T^{2.7} \exp(1250/T)$ cm^3/(mol s).[16]

Another influential process, which generates the NH_2 radical and H_2O, $OH + NH_3 \rightarrow NH_2 + H_2O$ (3), has been well established experimentally and theoretically over a broad temperature range.[21] k_3 exhibits a strong upward curvature above 1000 K. The existence of the curvature is consistent with our theoretically predicted result for the reverse process, $NH_2 + H_2O \rightarrow OH + NH_3$, $k_{-3} = 2.33 \times 10^3\ T^{2.94} \exp(-5566/T)$ cm^3/(mol s), computed with the transition state theory (TST) with tunneling corrections using the TS parameters obtained by a G2M/B3LYP/6-311G(d,p) calculation.[22] The expression for k_3 given in the mechanism was computed with the equilibrium constant $K_{-3} = 2.68 \times 10^{-2}\ T^{0.53} \exp(5846/T)$; it was used without adjustment.

The total rate constant and product branching ratios in reaction 4a used for this work were determined in this laboratory by laser-photolysis mass spectrometry (PLP/MS) over the temperature range of 300−990 K.[10] The rate constant is given by $k_4 = 8.10 \times 10^{16}\ T^{-1.44} \exp(-135/T)$ cm^3/(mol s) as a result from this study. The branching ratio for N_2O production, $\beta_{4b} = k_{4b}/(k_{4a} + k_{4b})$, β_{4b} was found to be independent of temperature, 0.19 ± 0.02, in the range investigated. This result agreed well with those reported by Hershberger et al., 0.14 ± 0.03[23] and 0.24 ± 0.03,[24] at room temperature and with that reached by kinetic modeling of the $NH_3 + NO_2$ reaction in the temperature range of 850−1350 K by Glarborg et al.[25] However, our result

TABLE 1: Key Reactions and Rate Constants[a] for the Kinetic Modeling of the Sublimed AN System

	reactions	*A*	*n*	*E*a	ref
1	$NH_4NO_3 = NH_3 + HNO_3$		sublimation		
2a	$HNO_3 + M = OH + NO_2 + M$	4.30×10^{03}	2.7	−2486	16
2b	$HNO_3 + (B_2O_3/SiO_2) = OH + NO_2 + (B_2O_3/SiO_2)$	7.91×10^{07}	0.0	25120	this work[b]
3	$NH_3 + OH = NH_2 + H_2O$	2.00×10^{06}	2.1	566	22
4a	$NH_2 + NO_2 = H_2NO + NO$	6.56×10^{16}	−1.5	268	10
4b	$NH_2 + NO_2 = N_2O + H_2O$	1.54×10^{16}	−1.5	268	10
5a	$NH_2 + NO = N_2H + OH$	1.43×10^{07}	1.4	−1776	9
5b	$NH_2 + NO = N_2+H_2O$	1.20×10^{17}	1.6	298	9
6	$OH + OH = H_2O + O$	2.11×10^{08}	1.4	−397	15
7	$OH + HNO_3 = H_2O + NO_3$	8.73×10^{00}	3.5	−1667	38
8	$OH + H_2NO = HNO + H_2O$	2.00×10^{07}	2.0	1000	10

[a] Rate constants, defined by $k = AT^n \exp(-E_a/RT)$, are given in units of cm^3, mol, and s; E_a is in units of cal/mol. [b] First-order rate coefficient.

was inconsistent with the large value of $\beta_{4b} = 0.59 \pm 0.03$ at room temperature reported by Meunier et al.[26]

We have also carried out a series of experiments for the determination of total rate constant and the branching ratios of the pivotal reactions 5a and 5b employing the PLP/MS technique covering a broad range of temperatures, 300−1200 K.[9] We determined the total rate constants for the reactions and their product branching ratios as $k_{5a} = 1.43 \times 10^7\ T^{1.40} \exp(894/T)$ and $k_{5b} = 1.20 \times 10^{17}\ T^{-1.61} \exp(-150/T)$ cm^3/(mol s). The kinetic data for product branching in reaction 5b, $NH_2 + NO$, can be represented as $\alpha_{5a} = 9.69 \times 10^{-3} - 1.31 \times 10^{-4}\ T + 3.96 \times 10^{-7}\ T^2 - 9.72 \times 10^{-11}\ T^3$ by a least-squares analysis of α_{5a} based on three different sets of our data (300−1200 K),[27] those of Glarborg and co-workers (1200 − 1370 K),[28] and those of Votsmeier et al. (1330−1670 K).[29]

Heterogeneous Decomposition of HNO_3. Nitric acid is the prototype of a sticky molecule having a significant residence time on all surfaces, and its values strongly depend on the experimental conditions and the type of technique employed. In 1951 Johnston and his co-workers[13] first studied the kinetics of the thermal decomposition of HNO_3 vapor in two glass cells of considerably different surface-to-volume ratios and an inner diameter of 6 or 25 mm with a length of 140 mm. All experiments were performed with about 5−25 torr of HNO_3 at a total pressure of 1 atm using nitrogen, oxygen, or carbon dioxide as a carrier gas in the temperature range of 373−738 K. The rate constants derived from their heterogeneous decomposition reactions are summarized in Figure 4 for comparison with our modeled values presented below. As shown in Figure 4, the decomposition rate was significantly dependent on the surface-to-volume ratio and insensitively on temperature below 573 K. However, there was a rapid change in the rate constant with temperature showing a first-order reaction above 700 K without any dependence on carriers gases used in their experimental conditions.

The heterogeneous decomposition reaction of HNO_3 on an amorphous carbon surface has been investigated by Thlibi and Petit in a static reactor at 303 K,[30] and they reported the decomposition of HNO_3 yields NO and NO_2 as products. Rogaski et. al[31] also reported that HNO_3 reacted heterogeneously on Degussa FW2 (an amorphous carbon black comprising medium oxides) leading to the formation of NO, NO_2, and H_2O. Recently Choi and Leu[32] studied extensively the decomposition of HNO_3 on Degussa FW2, graphite, hexane soot, and kerosene soot and reported that its decomposition rates strongly depend on the experimental conditions and the type of solid surface used. Significant HNO_3 decomposition was observed on FW2 and NO, NO_2, H_2O, and other unidentified volatile products were produced. Similar HNO_3 decomposition behavior on graphite was also observed, although the extent of the decomposition was much smaller than that on FW2. However, very little reactivity of HNO_3 was shown on hexane and kerosene soot surfaces. A fast heterogeneous decomposition of HNO_3 leading to NO_2, NO, H_2O, and O_2 was also observed by Rossi and his co-workers[33] in their study on the thermal decomposition of NH_4NO_3 using mass spectrometric detection of vapor-phase species and FTIR detection of condensable products. Theoretically, Parrinello and co-workers[34] studied the detailed heterogeneous interaction processes between gas-phase nitric acid and a graphite surface which led to the dissociation of the nitric acid and the production of NO_2 and OH radicals in the gas phase by ab initio molecular dynamics study at several different levels of density functional theory (DFT).[35]

Furthermore, different types of heterogeneous reactions of HNO_3 were studied by Rossi et al. They measured the reaction probability and surface residence time of HNO_3 on decane ($C_{10}H_{22}$) soot surface[36] and a series of salt powers (NaCl, NaBr, KCl, and KBr)[37] in a low-pressure flow reactor (Knudsen cell) using modulated molecular beam mass spectrometry for the quantification of reactant uptake and product release onto the gas phase. The heterogeneous reaction of HNO_3 with soot from a rich decane flame was proposed to be reduced to HONO as the main product, dependence on carrier gases formation of NO and NO_2; the latter also reacted on black soot to produce

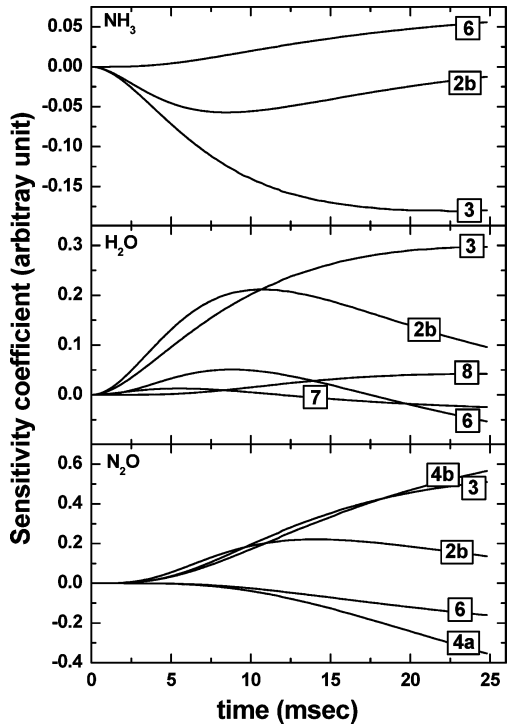

Figure 5. Sensitivity analysis at 952 K with $NH_3 = HNO_3 = 1.70$ mtorr, $N_2 = 0.07$ mtorr, $N_2O = 0.10$ mtorr, and $P = 6.2$ torr with He as carrier gas.

additional NO.[36] HNO_3 also showed stronger absorption on salt surfaces producing hydrogen halide as $HNO_3(g) + NaCl(s) \rightarrow HCl(g) + NaNO_3(s)$.[37]

As alluded to above, the homogeneous decomposition reaction of HNO_3 (2a) was far too slow and insufficient to initiate further chain reactions as observed experimentally. As shown in Figure 3 with dashed curves, no noticeable reactant decay or product formations were found. In order to account for the consumption of NH_3 and the formation of H_2O in our kinetic modeling (Figure 3), we take into consideration the heterogeneous decomposition of HNO_3 (2b) (see Table 1). The heterogeneous decomposition rate was determined by varying its rate to match the modeled yields of NH_3 and H_2O to experimentally measured concentrations. The values of k_{2b} are presented in Figure 4 together with Johnston's result[13] for comparison. Our results may be represented by $k_{2b} = 7.91 \times 10^7 \exp(-12\,600/T)\ s^{-1}$. In this work all experiments were performed with 1.7 and 2.3 mtorr of HNO_3 derived from AN decomposition at total pressures of 6.2 and 5.0 torr, respectively, using He as a carrier gas in the boric acid coated quartz tubular reactor tube with an inner diameter of 10 mm and a length of 70 mm as aforementioned. As shown in Figure 4, the heterogeneous decomposition rate of HNO_3 on the coated quartz surface was slightly faster than that on the glass surface at all temperatures studied (373−738 K) by Johnston and co-workers.[13] Interestingly, the extrapolation of Johnston's result agrees with our result in the high temperature range (>850 K).

Figure 5 presents the results of sensitivity analysis for the three major species measured, NH_3, H_2O, and N_2O at 952 K. Only reactions which are sufficiently influential (≥5% that of the most influential key process) are included in the figure. The sensitivity coefficient is defined as $S_{ij}(t) = \partial C_i(t)/\partial k_j \cdot k_j/C_i(t)$, where $C_i(t)$ is the concentration of species i at t and k_j is the rate constant of the jth reaction. The results of the sensitivity analysis show that the consumption of NH_3 and the formation of H_2O and N_2O products are strongly affected by the heterogeneous decomposition of HNO_3 (2b) and another important secondary reaction, $OH + NH_3 \rightarrow H_2O + NH_2$ (3), which has been described earlier in detail.

Summary

The absolute yields of NH_3, H_2O, N_2O, and N_2 measured in the thermal decomposition of AN, sublimed at 423 K below melting point, were kinetically modeled with a mechanism consisting of 115 reactions, assuming that the initial concentration of NH_3 is approximately equal to that of HNO_3. The mechanism employed was established through our earlier studies of the NH_x ($x = 2, 3$) + NO_y ($y = 1, 2$) systems, with the addition of the HNO_3 decomposition reaction whose rate constants were computed theoretically by means of *ab initio* MO/statistical theory calculations. In order to account for the fast overall decomposition reaction, the heterogeneous decomposition of HNO_3 has to be assumed in the mechanism; its rate constant determined by varying its rate constant to match the modeled result with the measured concentrations of NH_3 and H_2O could be reasonably represented by $k_{2b} = 7.91 \times 10^7 \exp(-12\,600/T)\ s^{-1}$. The kinetically modeled results with the heterogeneous initiation rate can satisfactorily account for the overall experimental product formation over the temperature range studied.

As mentioned in the Introduction, we had previously studied the kinetics of the thermal decomposition of ADN using the same apparatus;[3] the measured yields of NH_3, H_2O, N_2O, and N_2 could be reasonably accounted for with the homogeneous [H,N,O]-mechanism using our theoretically predicted $HN(NO_2)_2$ decomposition rate constant without invoking the heterogeneous initiation process as in the present AN case. The major difference between the two systems lies primarily in the higher stability of HNO_3 [$D(HO - NO_2) = 50$ kcal/mol][16] than that of $HN(NO_2)_2$ [$D(HN(NO_2) - NO_2 = 38$ kcal/mol].[3]

Acknowledgment. This work was supported by the Office of Naval Research under grant no. N00014-02-1-0133. M.C.L. gratefully acknowledges the support from Taiwan's National Science Council for a distinguished visiting professorship at the Center for Interdisciplinary Molecular Science, National Chiao Tung University, Hsinchu, Taiwan.

Supporting Information Available: The reactions and rate constants for the kinetic modeling of the sublimed AN system. This information is available free of charge via the Internet at http://pubs.acs.org.

References and Notes

(1) Rosser, W. A.; Inami, S. H.; Wise, H. *J. Phys. Chem.* **1963**, *67* (9), 1753.
(2) Brower, K. R.; Oxley, J. C.; Tewari, M. *J. Phys. Chem.* **1989**, *93*, 4029.
(3) Park, J.; Chakraborty, D.; Lin, M. C. *Proc. Combust. Inst.* **1998**, *27*, 2351–2357.
(4) Friedman, L.; Bigeleisen, J. *J. Chem. Phys.* **1950**, *18* (10), 1325.
(5) Rossi, M. J.; Bottaro, J. C.; McMillen, D. F. *Int J. Chem. Kinet.* **1993**, *25*, 549.
(6) Lyon, R. K. *Int. J. Chem. Kinet.* **1976**, *8*, 318; United States Patent 3,900,554.
(7) Wyatt, J. R.; De Corpo, J. J.; McDowell, M. V.; Saalfeld, F. E. *Rev. Sci. Instrum.* **1974**, *45*, 916. *J. Mass Spectrom. Ion Phys.* **1975**, *16*, 33.
(8) Park, J.; Lin, M. C. Technologies and Combustion for a Clean Environment. *Proc. 4th Int. Conf.* **1997**, *34−1*, 1–5.
(9) (a) Park, J.; Lin, M. C. *J. Phys. Chem.* **1996**, *100*, 3317–19. (b) Park, J.; Lin, M. C. *J. Phys. Chem. A* **1997**, *101*, 5–13.
(10) (a) Park, J.; Lin, M. C. *Int. J. Chem. Kinet.* **1996**, *28*, 879–883. (b) Park, J.; Lin, M. C. *J. Phys. Chem. A* **1997**, *101*, 2643–2647.

(11) Thaxton, A. G.; Hsu, C.-C.; Lin, M. C. *Int. J. Chem. Kinet.* **1997**, *29*, 245–251.
(12) Musin, R. N.; Lin, M. C. *J. Phys. Chem. A* **1998**, *102*, 1808.
(13) Johnston, H. S.; Foering, L.; Tao, Y.-S.; Messerly, G. H. *J. Am. Chem. Soc.* **1951**, *73*, 2319–21.
(14) (a) Donahue, N. M.; Dubey, M. K.; Morhschladt, R.; Demerjian, K. L.; Anderson, J. G. *J. Geophys. Res.* **1997**, *102*, 6159. (b) Gershenzon, Yu. M.; Dement'ev, A. P.; Nalbandyan, A. B. *Kinet. Catal.* **1979**, *20*, 565. (c) Smith, G. P.; Golden, D. M. *Int. J. Chem. Kinet.* **1978**, *10*, 489–501. (d) Glaenzer, K.; Troe, J. *Ber. Bunsen-Ges. Phys. Chem.* **1974**, *78*, 71. (e) Godfrey, T. S.; Hughes, E. D.; Ingold, C. J. *Chem. Soc.* **1965**,(f) Harrison, H.; Johnston, H. S.; Hardwick, E. R. *J. Am. Chem. Soc.* **1962**, *84*, 2478–2482.
(15) Tsang, W.; Herron, J. T. *J. Phys. Chem. Ref. Data* **1991**, *20*, 609.
(16) (a) Chakraborty, D.; Park, J.; Lin, M. C. *Chem. Phys.* **1998**, *231*, 39. (b) Zhu, R. S.; Lin, M. C. *J. Chem. Phys.* **2003**, *119* (20), 10667–10677.
(17) Doclo, K.; Roethlisberger, U. *Chem. Phys. Lett.* **1998**, *297*, 205.
(18) Houk, K. N.; Condroski, K. R.; Pryor, W. *J. Am. Chem. Soc.* **1996**, *118*, 13002.
(19) Sumathi, R.; Peyerhimhoff, S. D. *J. Chem. Phys.* **1997**, *107*, 1872.
(20) Mebel, A. M.; Morokuma, K.; Lin, M. C. *J. Chem. Phys.* **1995**, *103*, 7414.
(21) (a) Atkinson, R.; Baulch, D. L.; Cox, R. A.; Hampson, R. F., Jr.; Kerr, J. A.; Rossi, M. J.; Troe, J. *J. Phys. Chem. Ref. Data* **1997**, *26*, 1329–1499. (b) Corchado, J. C.; Espinosa-Garcia, J.; Hu, W.-P.; Rossi, I.; Truhlar, D. G. *J. Phys. Chem.* **1995**, *99*, 687–694. (c) Cohen, N.; Westberg, K. R. *J. Phys. Chem. Ref. Data* **1991**, *20*, 1211–1311. (d) Jeffries, J. B.; Smith, G. P. *J. Phys. Chem.* **1986**, *90*, 487. (e) Zabielski, M. F.; Seery, D. J. *Int. J. Chem. Kinet* **1985**, *17*, 1191. (f) Salimian, S.; Hanson, R. K.; Kruger, C. H. *Int. J. Chem. Kinet.* **1984**, *16*, 725.
(22) Mebel, A. M.; Moskaleva, L. V.; Lin, M. C. *THEOCHEM* **1999**, *223*, 461–462.
(23) Quandt, R.; Hershberger, J. *J. Phys. Chem.* **1996**, *100*, 9407.
(24) Lindholm, R.; Hershberger, J. *J. Phys. Chem. A* **1996**, *27,* 4991.
(25) Glarborg, P.; Dam-Johansen, K.; Miller, J. A. *Int. J. Chem. Kinet.* **1995**, *27*, 1207.
(26) Meunier, H.; Pagsberg, P.; Sillesen, A. *Chem. Phys. Lett.* **1996**, *261*, 277–282.
(27) Park, J.; Lin, M. C. *J. Phys. Chem. A* **1993**, *103*, 8906–07.
(28) Glarborg, P.; Kristensen, P. G.; Dam-Johansen, K.; Miller, J. A. *J. Phys. Chem. A* **1997**, *101*, 3741.
(29) Votsmeier, M.; Song, S.; Hanson, R. K.; Bowman, C. T. *J. Phys. Chem. A* **1999**, *103* (11), 1566.
(30) Thlibi, J.; Petit, J. C. In *Impact of Emissions from Aircraft and Spacecraft upon the Atmosphere*; Schumann, U., Wurzel, D., Eds.; Koln: Germany, 1994.
(31) Rogaski, C. A.; Golden, D. M.; Williams, L. R. *Geophys. Res. Lett.* **1997**, *24*, 381.
(32) Choi, W.; Leu, M.-T. *J. Phys. Chem. A* **1998**, *102*, 7618.
(33) Rossi, M. J.; Bottaro, Jeffrey C.; McMillen, D. F. *Int. J. Chem. Kinet.* **1993**, *25* (7), 549–70.
(34) (a) Rodriguez-Fortea, A.; Iannuzzi, M.; Parrinello, M. *J. Phys. Chem. C* **2007**, *111* (5), 2251–2258. (b) Rodriguez-Fortea, A.; Iannuzzi, M.; Parrinello, M. *J. Phys. Chem. B* **2006**, *110* (8), 3477–3484.
(35) (a) Becke, A. D. *J. Chem. Phys.* **1993**, *98*, 5648. (b) Becke, A. D. *J. Chem. Phys.* **1992**, *96*, 2155.
(36) Munoz, M. S. S.; Rossi, M. J. *Phys. Chem. Chem. Phys.* **2002**, *4* (20), 5110–5118.
(37) (a) Koch, T. G.; Van den Bergh, H.; Rossi, M. J. *Phys. Chem. Chem. Phys.* **1999**, *1* (11), 2687–2694. (b) Fenter, F. F.; Caloz, F.; Rossi, M. J. *J. Phys. Chem.* **1996**, *100* (3), 1008–1019.
(38) Xia, W. S.; Lin, M. C. *J. Chem. Phys.* **2001**, *114*, 4522–4532.

JP9058005